Supplementary Material (ESI) for *Polym. Chem.*

This journal is © The Royal Society of Chemistry

Effects of click postfunctionalization on thermal stability and field effect transistor performances of aromatic polyamines

Tsuyoshi Michinobu,*[,a,b] Chayeon Seo,[c] Keiichi Noguchi[d] and Takehiko Mori[c]

[a]*Global Edge Institute, Tokyo Institute of Technology, 2-12-1 Ookayama, Meguro-ku, Tokyo 152-8550, Japan*

[b]*Precursory Research for Embryonic Science and Technology (PRESTO), Japan Science and Technology Agency (JST), Honcho 4-1-8, Kawaguchi-shi, Saitama 332-0012, Japan*

[c] *Department of Organic and Polymeric Materials, Tokyo Institute of Technology, 2-12-1 Ookayama, Meguro-ku, Tokyo 152-8552, Japan*

[d] *Institute of Symbiotic Science and Technology, Tokyo University of Agriculture and Technology, Koganei, Tokyo 184-8588, Japan*

*Correspondence Address:

Dr. Tsuyoshi Michinobu

Global Edge Institute, Tokyo Institute of Technology

2-12-1 Ookayama, Meguro-ku, Tokyo 152-8550, Japan

Tel/Fax: +81-3-5734-3774, E-mail: michinobu.t.aa@m.titech.ac.jp

1. ^{1}H NMR

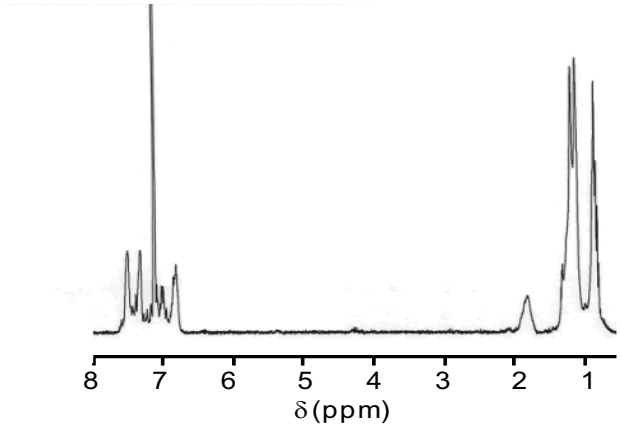

Fig. S1 ^{1}H NMR spectrum of **P4** (x = 1) in $CDCl_3$ at 20 ^{o}C.

2. MALDI-TOF mass

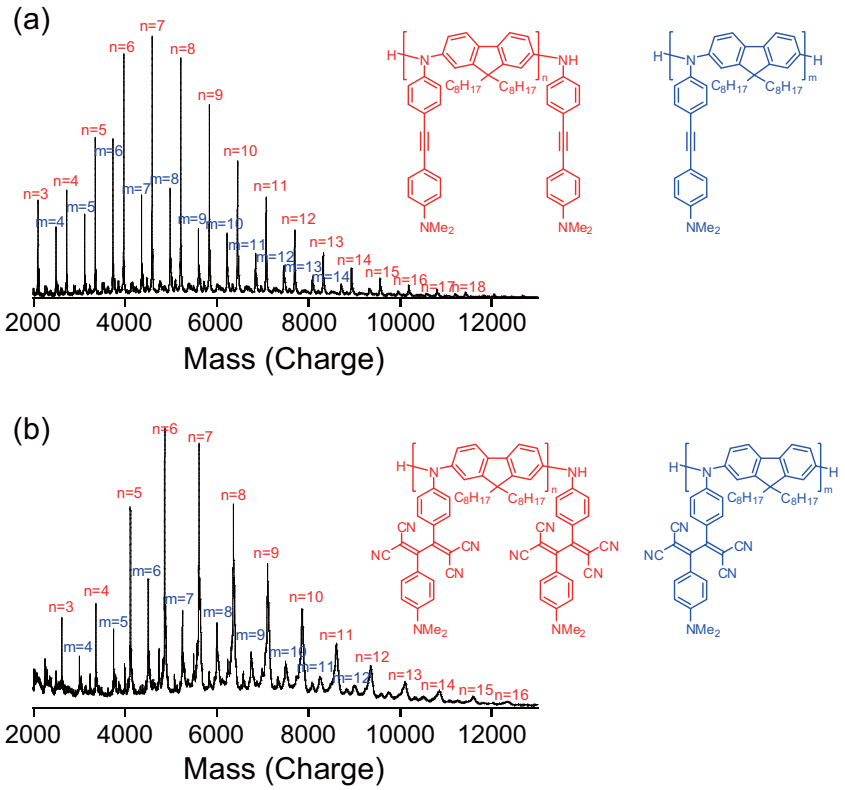

Fig. S2 MALDI-TOF mass spectra of (a) **P1** and (b) **P3** (x = 1) (matrix: dithranol).

3. IR spectra

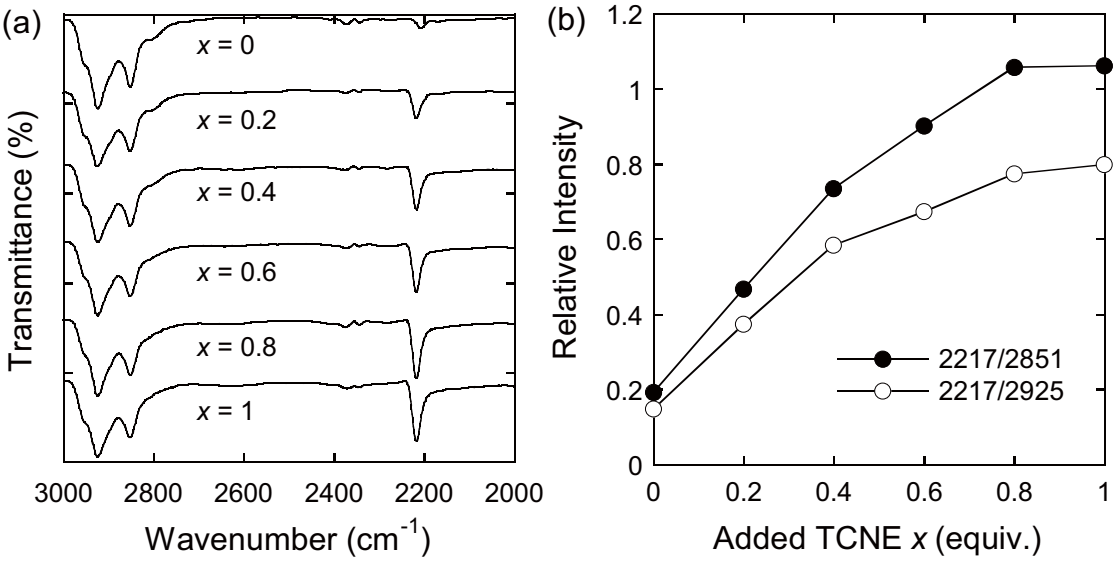

Fig. S3 (a) IR spectra (KBr) of **P1** and **P3** with different added TCNE amounts *x* and (b) plots of *x* values and the relative intensities of alkyl vibrational peaks at 2925 or 2851 cm^{-1} and C≡C + C≡N peak at 2217 cm^{-1}.

4. UV-Vis absorption spectra

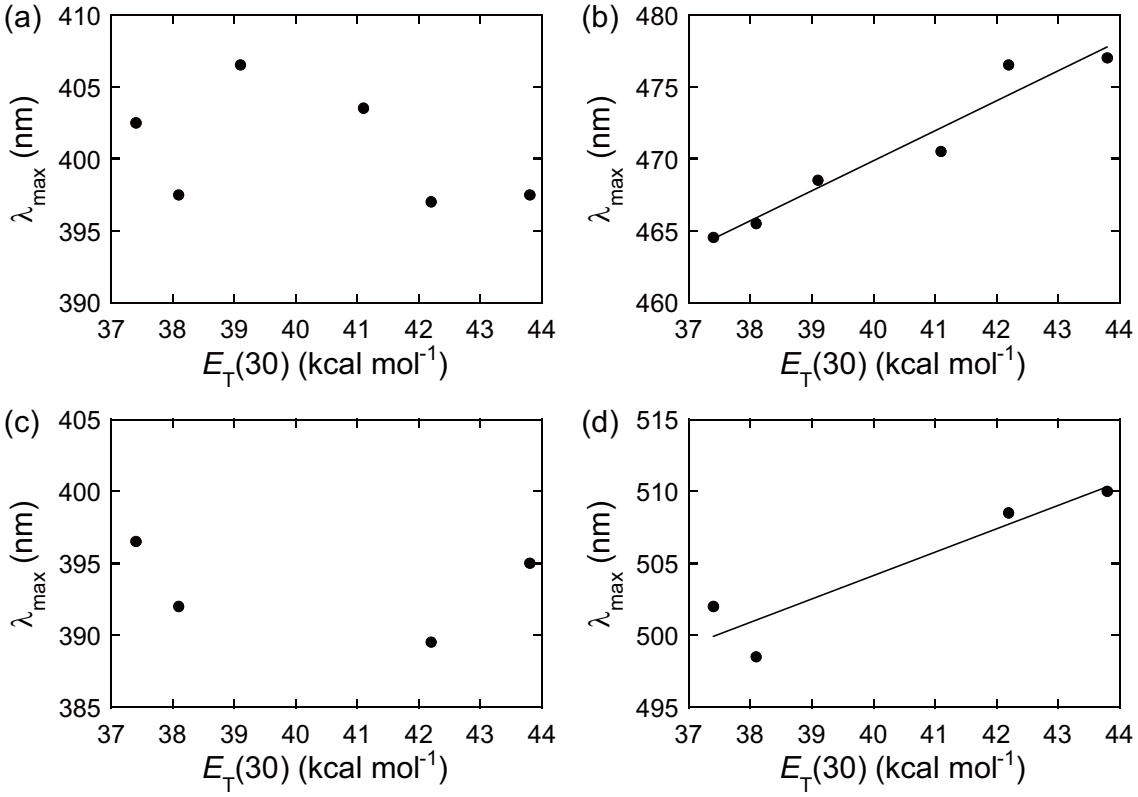

Fig. S4 Relationship between the solvent polarity parameter $E_T(30)$ (tetrahydrofuran, 37.4; ethyl acetate, 38.1; chloroform, 39.1; dichloromethane, 41.1; acetone, 42.2; *N*,*N*-dimethylformamide, 43.8) and the λ_{max} values of (a) **P1**, (c) **P2**, (b) **P3** (x = 1), and (d) **P4** (x = 1).

5. Thermal analyses

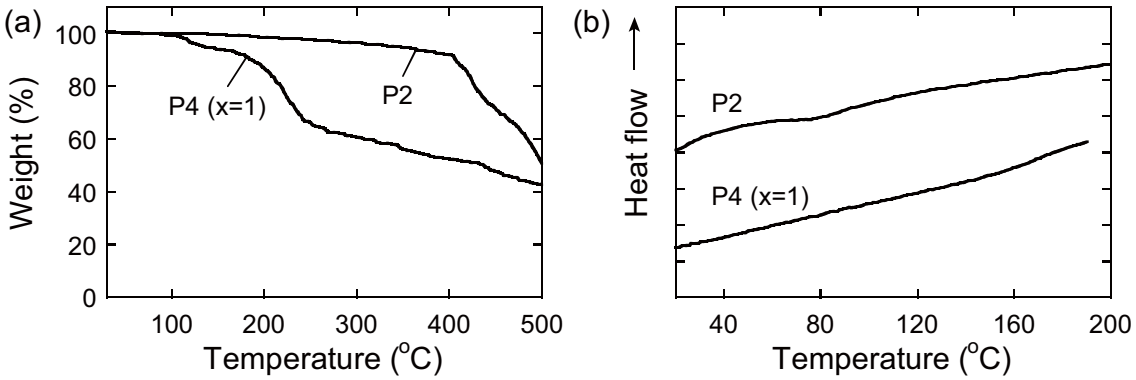

Fig. S5 (a) Thermogravimetric analysis (TGA) curves and (b) differential scanning calorimetry (DSC) curves of **P2** and **P4** (x = 1) at the scanning rate of 10 ^{o}C min^{-1} under flowing nitrogen.

6. Electrochemistry

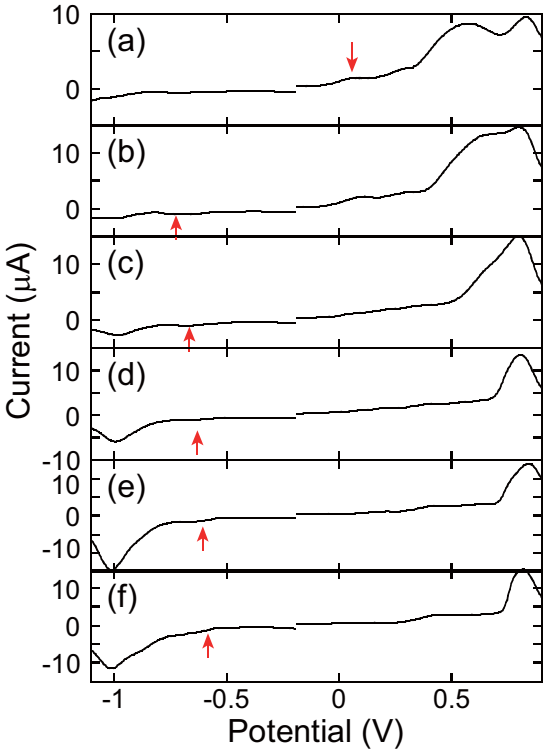

Fig. S6 Differential pulse voltammograms of (a) **P1**, (b) **P3** (x = 0.2), (c) **P3** (x = 0.4), (d) **P3** (x = 0.6), (e) **P3** (x = 0.8), and (f) **P3** (x = 1) in CH_2Cl_2 containing 0.1 M $(n C_4H_9)_4NClO_4$ at 20 °C.

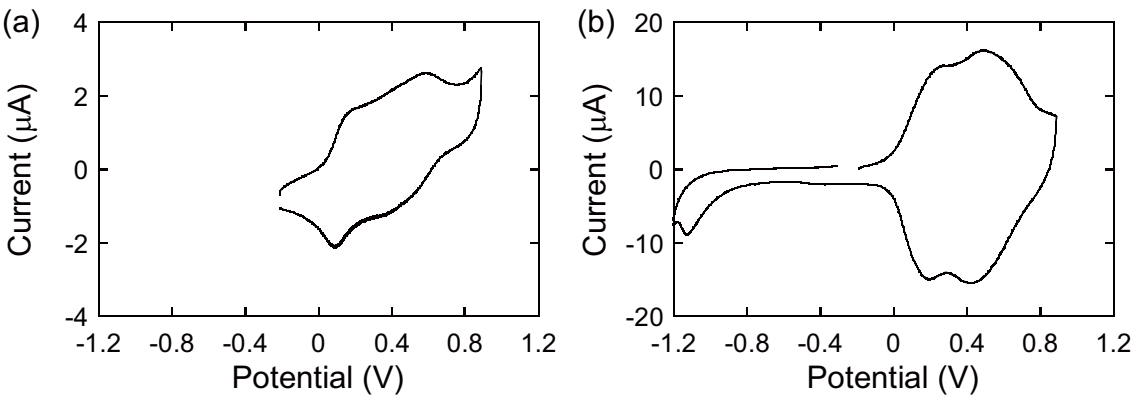

Fig. S7 Cyclic voltammograms of (a) **P2** and (b) **P4** (x = 1) in CH_2Cl_2 containing 0.1 M $(n C_4H_9)_4ClO_4$ at 20 °C.

Table S1 Summary of optical and electrochemical data of **P2** and **P4**.

	$E_{ox,1}$ or $E_{red,1}$ (V)[a]	LUMO (eV)	HOMO (eV)	λ_{end} (nm [eV])[b]
P2	+0.030	-1.970	-4.830	433 [2.86]
P4 (x = 1)	-0.930	-3.870	-5.470	775 [1.60]

[a] Determined by the onset oxidation or reduction potentials of cyclic voltammograms (vs. Fc/Fc^+).
[b] In CH_2Cl_2.
[c] Calculated from the HOMO and the optical band gap.
[d] Calculated from the LUMO and the optical band gap.

7. Atomic force microscopy (AFM) images

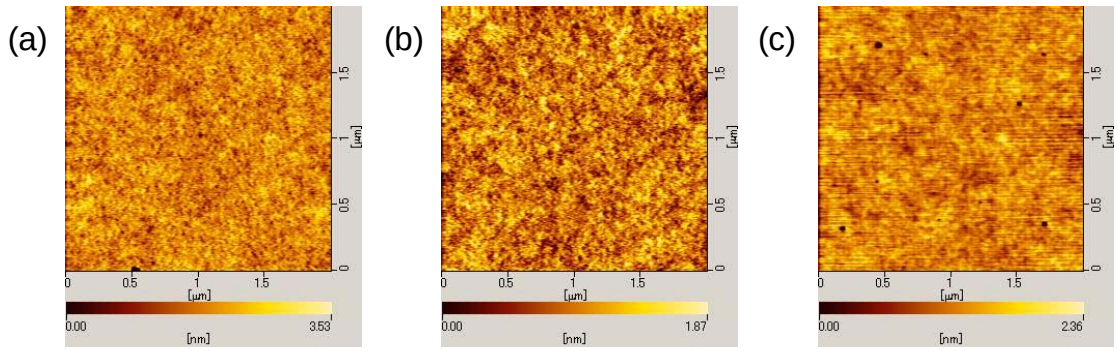

Fig. S8 AFM images (2.0 × 2.0 µm^2) of (a) **P1**, (b) **P3** (x = 0.2), and (c) **P3** (x = 0.4) films prepared on a Si/SiO_2 substrate by spin-coating at 5000 rpm for 60 s.